Science Signaling
AAAS

stke.sciencemag.org/cgi/content/full/14/676/eaaz2120/DC1

Supplementary Materials for

Inositol 1,4,5-trisphosphate 3-kinase B promotes Ca^{2+} mobilization and the inflammatory activity of dendritic cells

Laura Marongiu, Francesca Mingozzi, Clara Cigni, Roberta Marzi, Marco Di Gioia, Massimiliano Garrè, Dario Parazzoli, Laura Sironi, Maddalena Collini, Reiko Sakaguchi, Takashi Morii, Mariacristina Crosti, Monica Moro, Stéphane Schurmans, Tiziano Catelani, Rany Rotem, Miriam Colombo, Stephen Shears, Davide Prosperi, Ivan Zanoni, Francesca Granucci*

*Corresponding author. Email: francesca.granucci@unimib.it

Published 30 March 2021, *Sci. Signal.* **14**, eaaz2120 (2021)
DOI: 10.1126/scisignal.aaz2120

This PDF file includes:

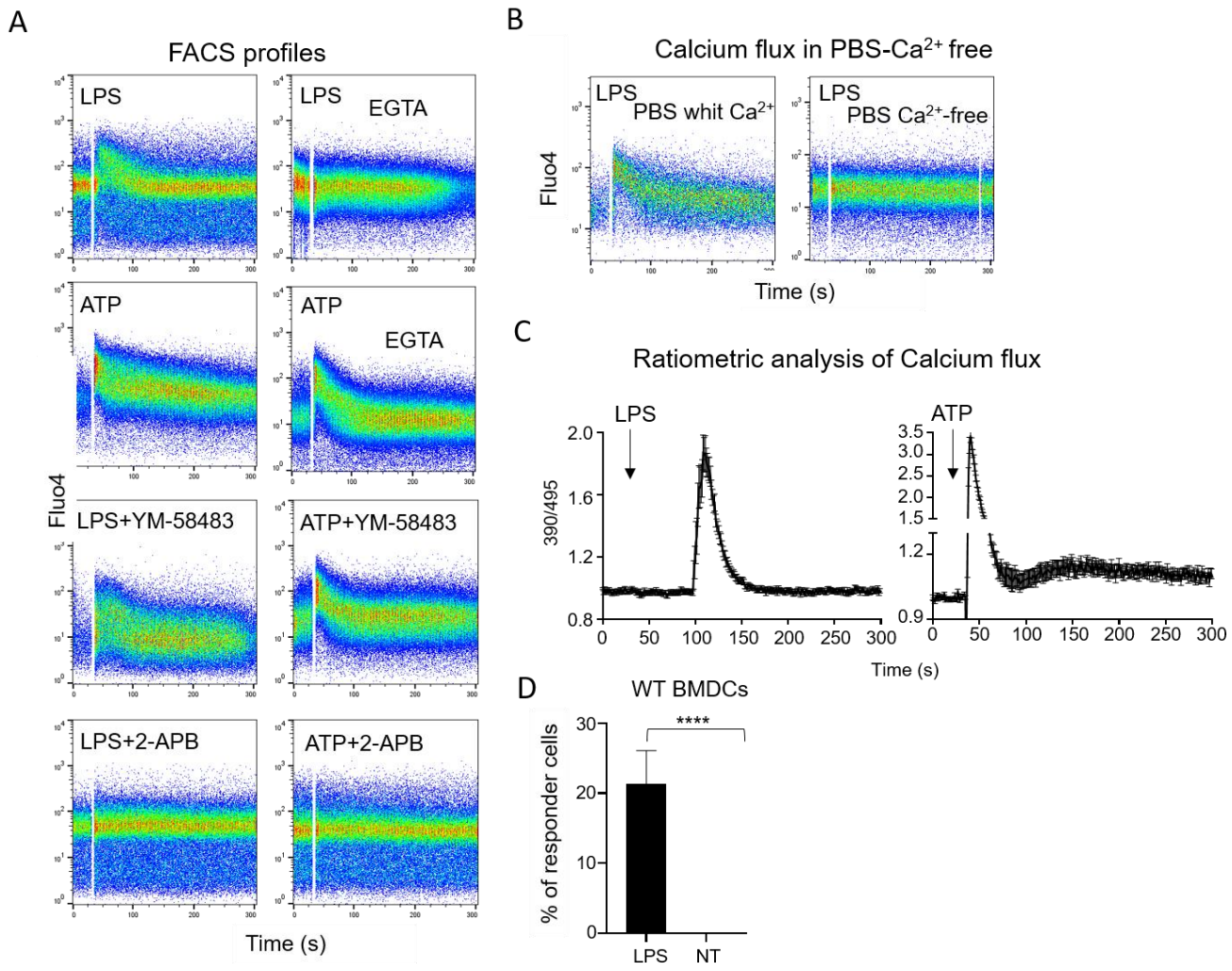

Fig. S1. Ca^{2+} fluxes in D1 cells in response to LPS stimulation measured by flow cytometry or with a ratiometric method. (**A**) Ca^{2+} flux profiles obtained by flow cytometry presented as dot plots showing fluo-4 raw fluorescence of the bulk population over time at the indicated conditions. These data are reported as relative fluorescence analysis in the main text (Fig. 1A). Each dot represents a single cell. (**B**) Ca^{2+} flux profiles obtained by flow cytometry in D1 cells treated with LPS (1µg/mL) in medium containing Ca^{2+} or in Ca^{2+}-free medium. The dot plots show fluo-4 raw fluorescence of the bulk population over time at the indicated conditions. (**C**) Ca^{2+} flux profiles obtained by a ratiometric method. D1 cells were loaded with indo-1 and analyzed with confocal microscopy. Arrows indicate the time (30 s) of LPS (1µg/mL) or ATP (100µM) administration. $[Ca^{2+}]i$ transients were evaluated as the fluorescence change in the 390/495 nm ratio, in response to the stimuli. Plots show the profile of 35 cells. (**D**) Percentage of BMDCs that mobilize calcium in response to LPS (1µg/mL) stimulation compared to untreated cells (NT). Calcium response were evaluated and measured by flow cytometry. Data represent 4 independent experiments. Statistical significance was determined with unpaired student's *t*-test. **** $P<0.0001$.

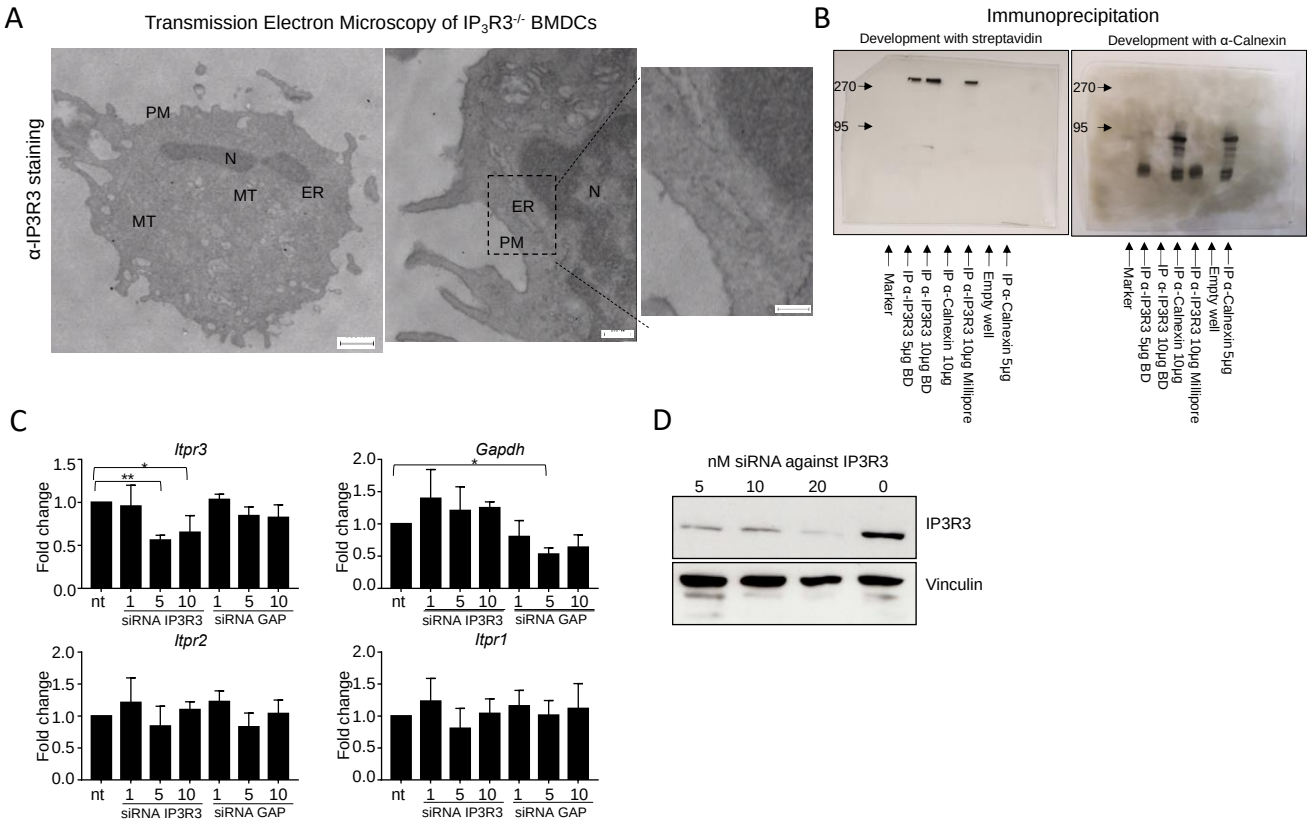

Fig. S2. IP_3R3 localization on the plasma membrane and IP_3R3 knockdown. (**A**) TEM of IP_3R3-deficient mouse BMDCs labelled to show IP_3R3. Representative image shows whole BMDCs. ER, endoplasmic reticulum; MT, mitochondria; N, Nucleus; PM, plasma membrane. Images are representative of 2 independent analyses. Scale bars, 300nm (left), 200 nm (middle), 50nm (right). (**B**) Original western blots presented in Fig. 2D of the main text. (C) Efficiency of IP_3R3 knock down. *ITPR3*, *ITPR2*, *ITPR1* and *GAPDH* expression in D1 cells treated with the indicated amounts of siRNAs targeting IP_3R3. siRNAs against GAPDH were used as control. Data represent 3 independent experiments. Statistical significance was determined with one-way analysis of variance followed by Sidak's multiple comparison test. ** $P<0.01$, * $P<0.05$. (**D**) Western blots for IP_3R3 in D1 cells transfected with the indicated amounts of siRNAs targeting IP_3R3. Vinculin is a loading control. Data are representative of 2 independent experiments.

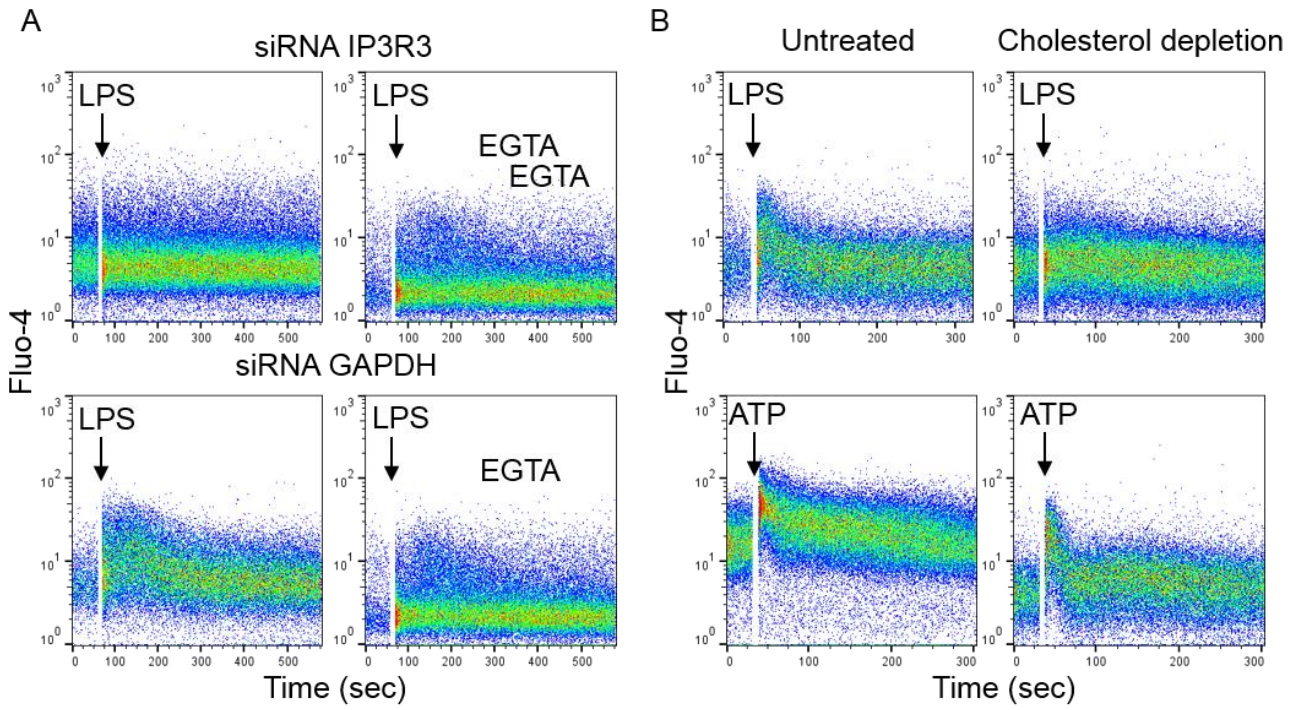

Fig. S3. Flow cytometry analysis of Ca^{2+} fluxes. Ca^{2+} flux profiles obtained by flow cytometry reported as relative fluorescence analysis in the main text. Dot plots showing fluo-4 raw fluorescence of the bulk population over time at the indicated conditions are relative to the samples presented in (**A**) Fig. 3A and (**B**) Fig. 4D. Each dot represents a single cell.

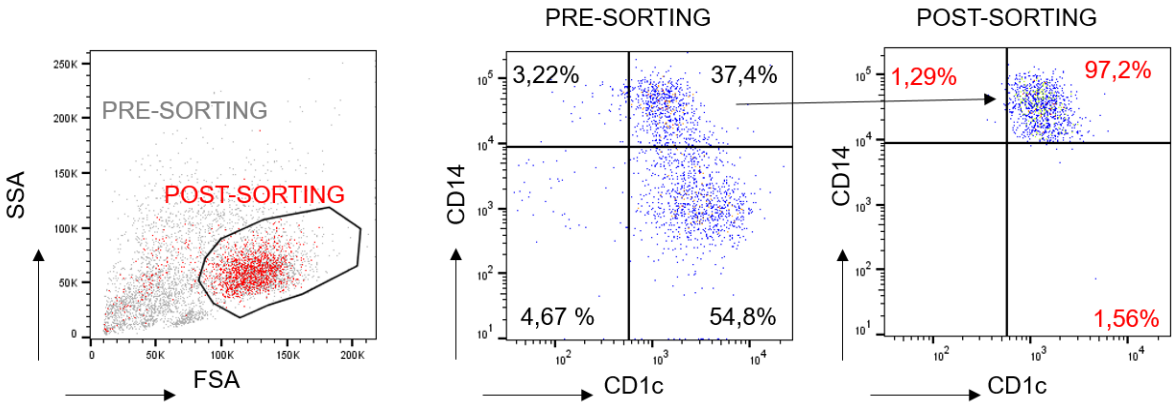

Fig. S4. Sorting strategy of DC3 cells. $CD1c^+$ ($BDCA1^+$) cells were purified from buffy coats using magnetic sorting (pre-sorting). $CD1c^+CD14^+$ cells were then obtained by FACS sorting (post-sorting). Panels show the physical parameters and CD14 and CD1c expression on the pre-sorted and post-sorted cells.

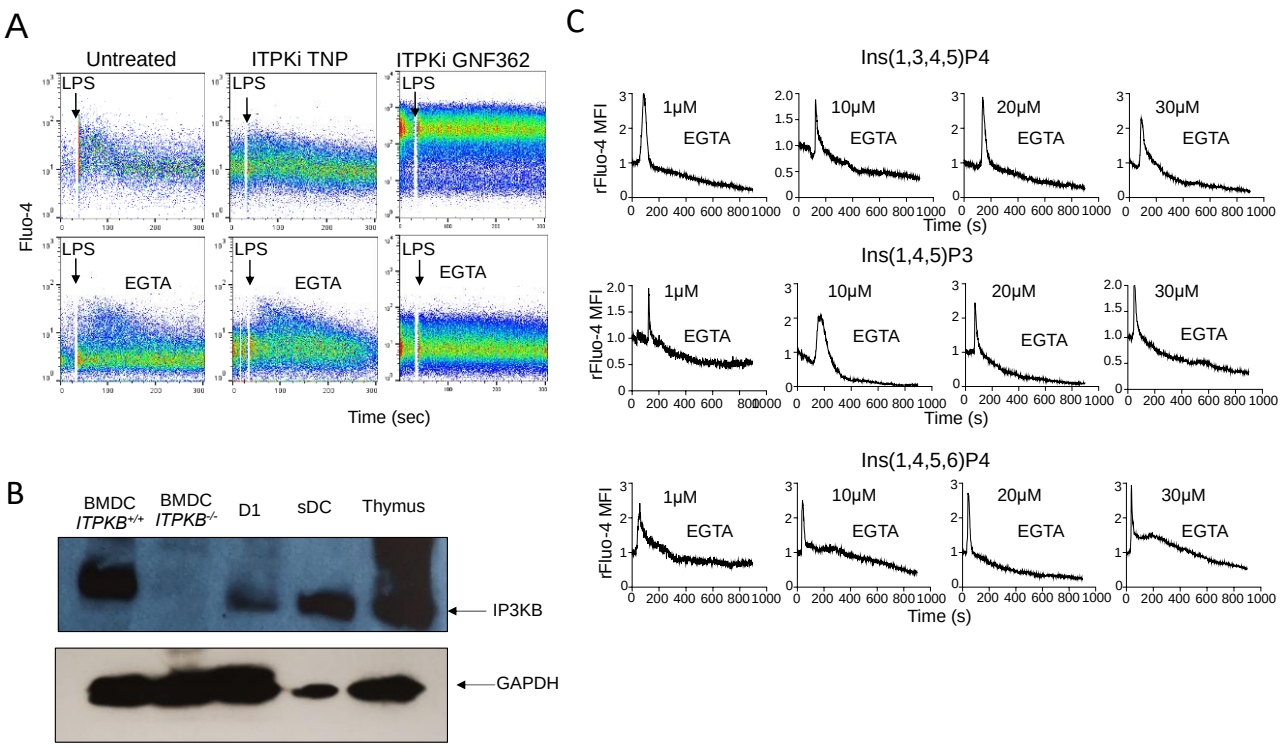

Fig. S5. ITPKB in DCs and role in Ca^{2+} mobilization in response to LPS.
(**A**) Ca^{2+} flux profiles obtained by flow cytometry presented as dot plots showing fluo-4 raw fluorescence of the bulk population over time at the indicated conditions. These data are reported as relative fluorescence analysis in the main text (Fig. 5A). Each dot represents a single cell. (**B**) Western blot showing ITPKB and GAPDH in BMDCs derived from WT and ITPKB-deficient mice, D1 cells, WT spleen DCs (sDC), and thymus (positive control). (**C**) Representative Ca^{2+} profiles of DCs pretreated with the CRAC inhibitor YM-58483, then treated with thapsigargin (TPG) to deplete the intracellular Ca^{2+} stores, and finally with cell-permeant Ins(1,3,4,5,)P_4, Ins(1,4,5)P_3, or Ins(1,4,5,6)P_4 at the indicated doses, in the presence of EGTA. TPG was added after 30 s and inositols after 600s of data acquisition. Ca^{2+} fluctuations were evaluated as changes in Fluo-4 fluorescence in response to the stimuli and normalized over the first 30s of analysis (rFluo-4MFI). Data are representative of n = 3 independent experiments.

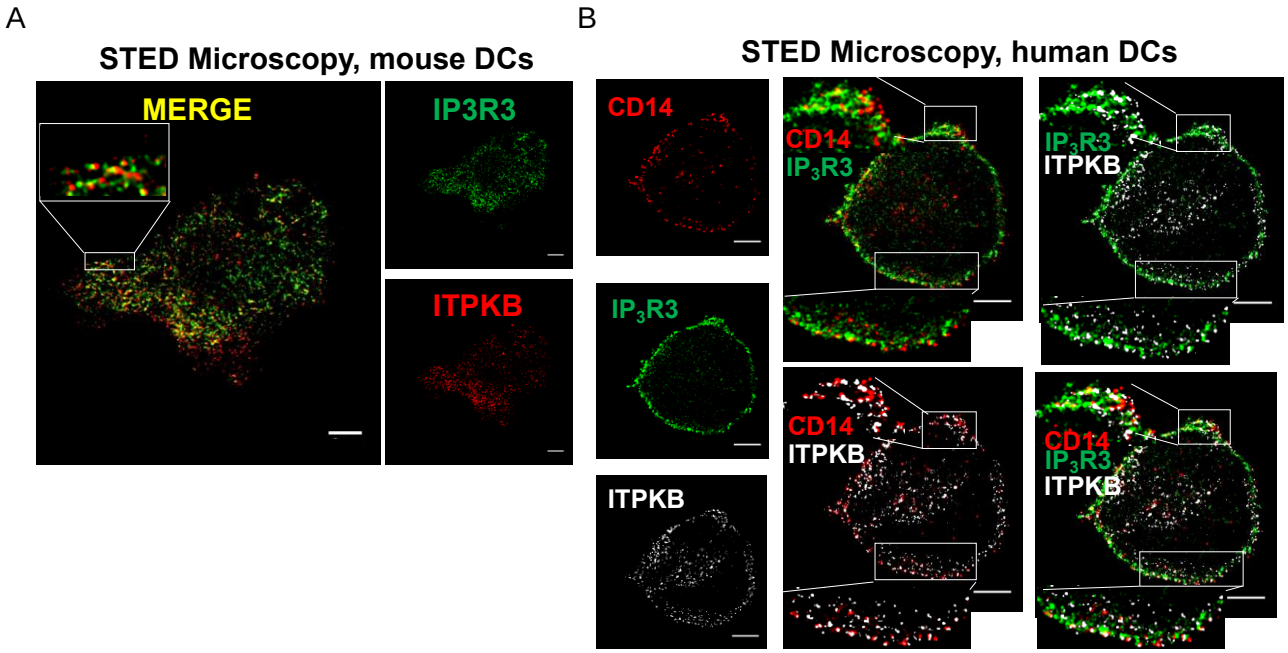

Fig. S6. Colocalization of IP_3R3, CD14, and ITPKB in DCs. (**A**) STED microscopy showing ITPKB (red) and IP_3R3 (green) in mouse D1 cells. antibodies. Scale bars, 2μm. Images are representative of 5 independent analyses. (**B**) STED microscopy showing IP_3R3 (green), CD14 (red), and ITPKB (white) in human $CD1c^+CD14^+$ cells. Scale bars, 2μm. Images are representative of 5 independent analyses from 2 donors.

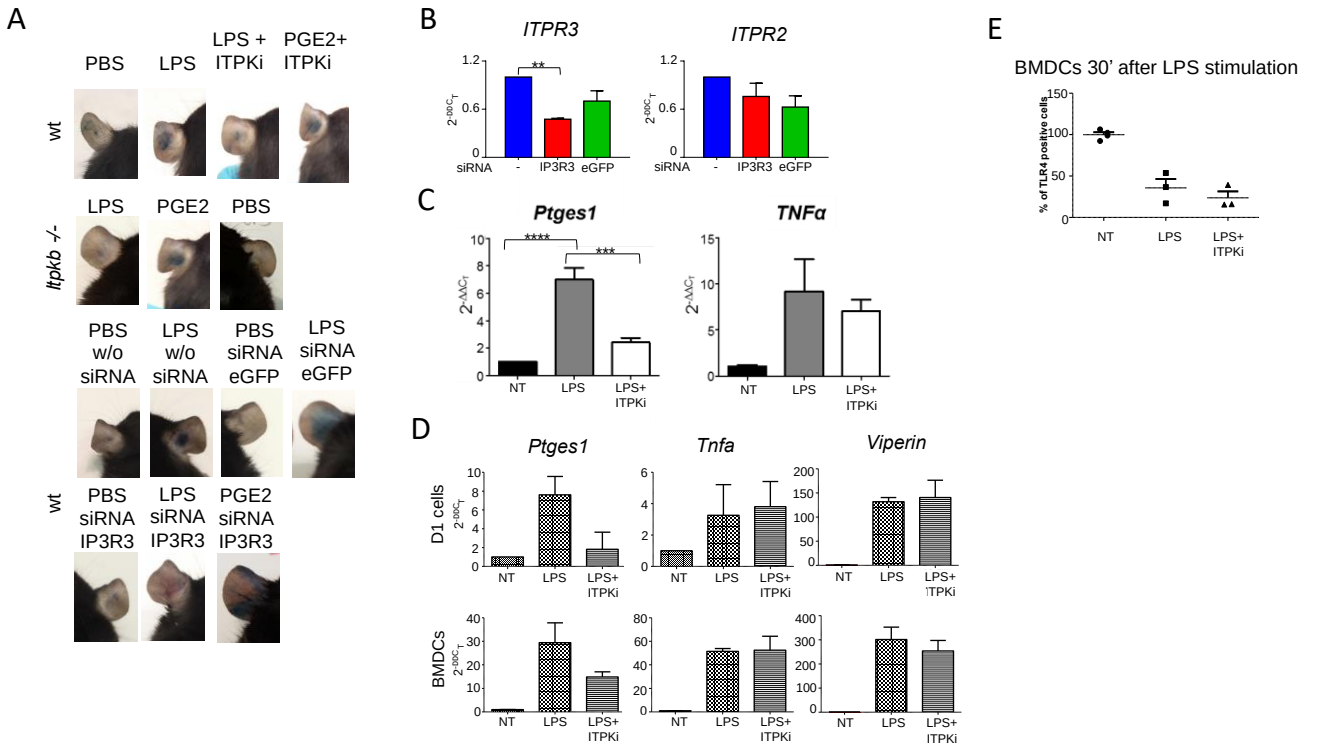

Fig. S7. ITPKB is required for LPS-induced vascular leakage. (**A**) Representative images of vascular leakage assayed by Evans blue extravasation in the ears. WT and ITPKB-deficient (*Itpkb*$^{-/-}$)mice were simultaneously injected i.v. with Evans blue and subcutaneously injected with the indicated combinations of PBS, LPS, TNP (ITPKi), and PGE_2. A group of mice was also pre-treated with siRNAs specific for IP3R3 siRNA 24 hours before to the vasodilation test. (**B**) Efficiency of siRNA-mediated IP_3R3 knockdown in vivo. *ITPR3* and *ITPR2* expression was quantified 24h after ear subcutaneous injection of anti-IP_3R3 siRNAs. siRNAs against eGFP were used as a negative control. Data represent 3 independent experiments. Statistical significance was determined with one-way analysis of variance followed by Sidak's multiple comparison test. ** P<0.01, * P<0.05. (**C**) Real-time PCR analysis of *Ptges1* and *Tnfa* expression in ear tissues of mice 4h after subcutaneously injected or not (nt) with LPS in the presence or absence of TNP (ITPKi). Values represent mean ± SD of 4 independent experiments. Statistical significance was determined with one-way analysis of variance followed by Tukey's multiple comparison test. ** P<0.01. (D) *Ptges* (NFAT-dependent), *Tnfa* (MyD88-dependent), and *Viperin* (TRIF-dependent) expression in mouse D1 cells and BMDCs 4h after LPS activation. NT, not treated. Where indicated cells, were co-treated with LPS and TNP (ITPKi). Values represent mean ± SD of 3 independent experiments. (**E**) Quantification of surface TLR4 on BMDCs 30 min after LPS treatment in the presence or not of the TPG (ITPKi). Values represent the mean of 3 independent experiments.

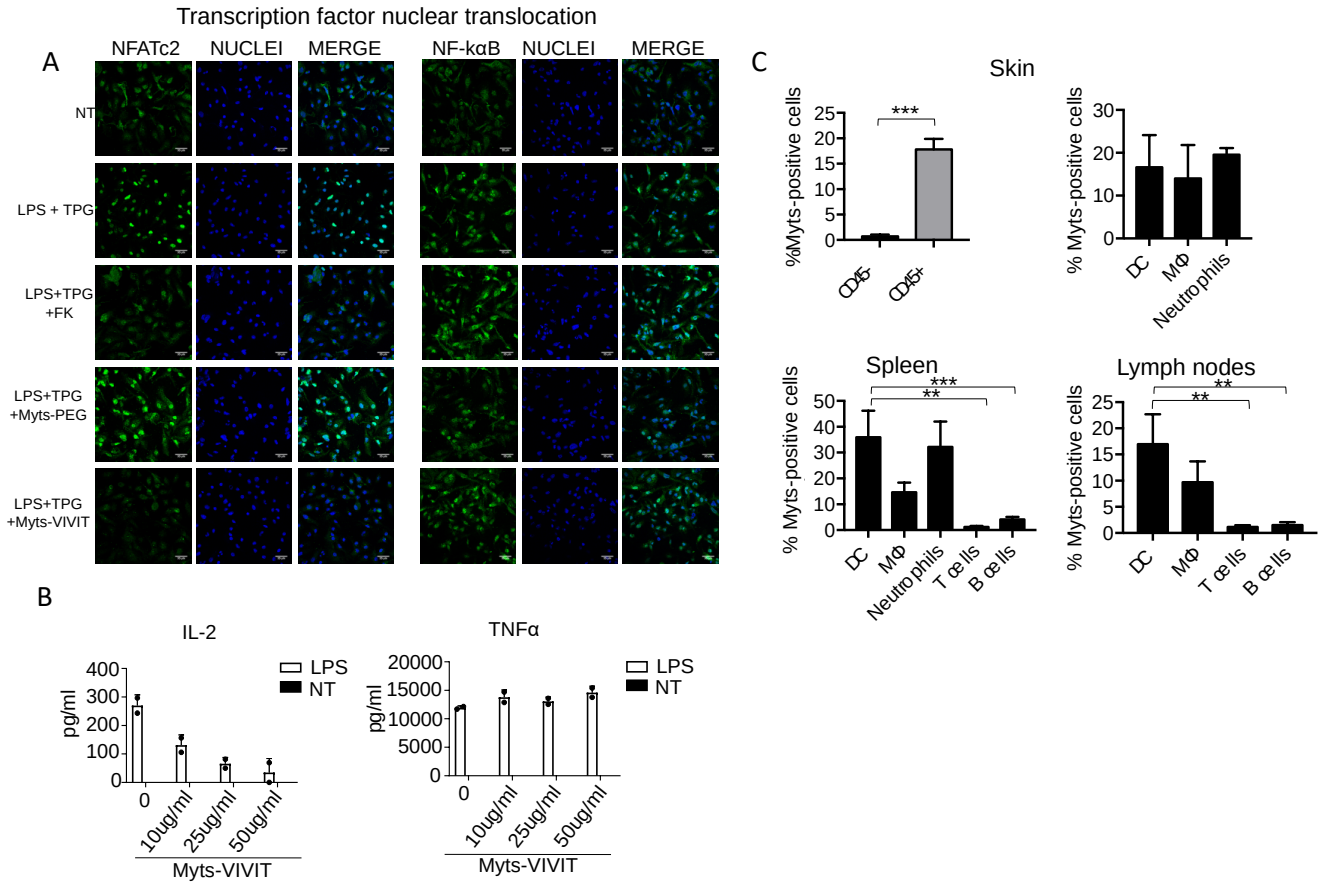

Fig. S8. Inhibition of nuclear NFAT translocation by Myts-VIVIT nanoparticles. (**A**) Confocal microscopy analysis of nuclear NFAT and NF-κB (p65) translocation induced in mouse BMDCs by LPS and thapsigargin (TPG). Where indicated, the cells were pretreated with FK506, Myts-VIVIT, or MyTS-PEG prior LPS and TPG treatment. (**B**) Quantification of IL-2 (NFAT-dependent) and TNF-α (NFAT-independent) production by BMDCs after stimulation with LPS in the presence or not of the indicated amounts of Myts-VIVIT. (**C**) In vivo uptake of FITC-conjugated Myts nanoparticles. Fluorescent Myts were injected i.v. every other day for two weeks and half (Days 1, 3, 5, 8, 10, 12, 17), and FITC-positive cells in the skin, lymph nodes, and spleen were counted by FACS analysis at Day 18. Values represent mean ± SD of 3 independent experiments. Statistical significance was determined with unpaired student's *t*-test or one-way analysis of variance followed by Tukey's multiple comparison test. ** P<0.01. *** P<0.0001.